

Rhodamine-Labeled LDL as a Tool to Monitor the Lipoprotein Traffic in Experimental Model of Early Atherosclerosis in Mice

DYAH SAMTI MAYASARI¹, NORIAKI EMOTO^{1,2,*}, KEIKO YAGI²,
NICOLAS VIGNON-ZELLWEGER², KAZUHIKO NAKAYAMA²,
TETSUYA MIYOSHI³, OKIKO MIYATA³, and KEN-ICHI HIRATA¹

*1*Division of Cardiovascular Medicine, Department of Internal Medicine, Kobe University Graduate School of Medicine, Kobe, Japan; *2*Clinical Pharmacy and *3*Medicinal Chemistry, Kobe Pharmaceutical University, Kobe, Japan *Corresponding author

Received 14 February 2013/ Accepted 15 February 2013

Key words: Rhodamine B NHS ester, LDL retention, Carotid ligation, Intimal thickening, Atherosclerosis

Modifications of proteoglycans, subendothelial retention of low-density lipoproteins (LDL) and their subsequent oxidation initiate the development of atherosclerosis. Therefore, detection of lipoprotein entrapment in the arterial wall is an important feature for the analysis of the mechanisms of atherosclerosis. The administration of fluorescent-labeled LDL in vivo is a breakthrough way to assess the traffic of LDL in the arterial wall. The present study demonstrated the feasibility of visualizing LDL in carotid ligation-induced intimal thickening of arterial wall after intravenous rhodamine-labeled LDL injection in mice. Kinetics of rhodamine-labeled LDL showed similar characteristics as native LDL and labeled-LDL could be detected both by spectrophotometric and microscopic analysis. Kinetics analysis of rhodamine-labeled LDL revealed that the labeled LDL was present in almost all tissue, predominantly in the liver, 6 hours after injection. Rhodamine-labeled LDL was visualized in intimal thickening of carotid 6 to 18 hours after injection, indicating that the LDL was actively trapped in the arterial wall. In conclusion, rhodamine-labeled LDL would be a useful tool to investigate the development of atherosclerosis.

Retention of lipoproteins, such as low-density lipoproteins (LDL), in the arterial wall is an important mechanism in the development of atherosclerosis. One hypothesis, known as “response-to-retention” hypothesis, states that LDL are trapped in diffuse intimal thickening (DIT) of the arterial wall. In this early stage of atherosclerosis, LDL would bind to the extracellular matrix on proteoglycans (PGs)(1). In vitro studies suggest that the elongation of chondroitin sulfate (CS) chains on PGs is essential for PGs to bind LDL (2-5). Recently we showed that CS chains were elongated during the development of atherosclerosis in LDL receptor knockout mice (6). Thus, inhibition of LDL trapping in the arterial wall represents a potential strategy for the treatment of atherosclerosis. To investigate the role of LDL trapping during the initiation process of atherosclerosis, we need a method that clearly monitors the traffic of lipoprotein through the arterial wall. For decades, labeled LDL has been a tool for the assessment of tissue distribution and degradation of LDL. Studies using radioisotopes and fluorescent labeled lipoproteins have provided a huge contribution for the

RHODAMINE-LABELED LDL FOR MONITORING LIPOPROTEIN TRAFFIC

observation of cellular binding and uptake of lipoproteins in culture dishes as well as in animal models. Iodine-125 (^{125}I) is one of the radioisotopes which is widely used to label LDL (7, 8). Nowadays, fluorescent dyes are used preferentially to label LDL, because of their lower cost, ease of disposal, similar sensitivity to radioisotopes, feasibility of multicolor labeling, and finally for their easy detection by fluorescent imaging devices (9). Rhodamine is a fluorescent compound commonly used in biological applications, including for labeling proteins and nucleic acids. The fluorescence of rhodamine is pH independent, photo- and chemically stable. Moreover, its excitation and emission wavelengths (500-600 nm) are within a range where the autofluorescence of cells is negligible (10, 11). Rhodamine-labeled LDL has been used to observe the lipoprotein distribution in various tissues (12-15). However, until now rhodamine-labeled LDL has not been used to monitor early atherosclerosis process in mice.

In this paper, we investigated the feasibility to detect arterial lipoprotein retention in a mouse model of intimal thickening using rhodamine-labeled LDL which was prepared by conjugation of rhodamine B NHS (N-hydroxysuccinimidyl) ester with LDL. This method may have potentials as a prognostic tool to identify whether the arterial wall is atherosclerosis-prone and as a monitoring tool to investigate the role of LDL during development of atherosclerosis.

MATERIAL AND METHODS

Lipoprotein preparation

LDL (density=1.020 to 1.063) was isolated by differential ultracentrifugation of EDTA-plasma from healthy donor. LDL was dialyzed against PBS, sterilized through 0.45 μm filters and kept at 4°C. Concentration of purified LDL was measured by Bradford analysis.

Lipoprotein labeling

The labeling protocol of LDL was modified from a previous one (16). Rhodamine B NHS ester (prepared by Medicinal Chemistry, Kobe Pharmaceutical University, Kobe, Japan) was diluted in DMSO at 10 mg/ml. LDL (2 mg/ml) was dissolved in fresh 0.1M sodium bicarbonate pH 8.3 before stirring with 1 mg amine-reactive rhodamine B NHS ester for 1 hour. Hydroxylamine 1.5M pH 8.5 was used to stop the binding reaction. Free dyes were removed by filtering the solution in sephadex G-25 equilibrated with phosphate buffered solution (PBS). Rhodamine-labeled LDL was kept in the dark in 0.01% NaN_3 at 4°C. Labeling of LDL was confirmed by electrophoresis using 1% agarose gel (universal gel/8, Helena Laboratories, Saitama, Japan). Conditions for electrophoresis were 90V for 1 hour at room temperature. Rhodamine-labeled LDL were visualized on the gels under UV light and photographed. Finally, the gels were stained for total protein detection with Coomassie Brilliant Blue R-250 (ICN Biomedicals, Ohio).

Animal experiment

The use of animals in the present study was approved by the Animal Facility of Kobe Pharmaceutical University, Kobe, Japan. Eight weeks old male C57BL/6Jc1 mice (n=44, 20-25 g, CLEA Japan) were anesthetized by inhalational isoflurane (Merck). The left common carotid artery was ligated near bifurcation with the use of 7-0 silk (Akiyama Seisakusyo, Japan). The wound was sutured, and animals were fed standard CRF-1 mouse chow (Charles River Laboratories International, Inc., Wilmington, MA) for two weeks. Injection of rhodamine-labeled LDL (~300 μg) was performed intravenously through the femoral vein under isoflurane anesthesia. Mice which didn't receive any injection or an injection with unbound rhodamine B NHS ester were used as negative controls. Mice were

sacrificed 1 and 30 minutes, 2, 6, 12, 18, 24 and 50 hours after injection. Serum and organs (liver, adipose tissue, kidney, aorta, and heart) were collected. Tissues were frozen in liquid nitrogen and kept at -80°C until analysis. Carotid artery, liver, heart and lymph node were fixed in 4% PFA for 2 hours then dehydrated with 30% sucrose before to be frozen in OCT compound.

Fluorescence assay

Tissues were homogenized in phosphate buffered saline by using a glass homogenizer (Wheaton) for aorta and polytron homogenizer PT3100 (Polytron Kinematica, USA) for liver, adipose tissue, kidney and heart. Homogenized samples were applied in duplicate in 96-well plates. Relative fluorescence units were measured with a Fluoromark microplate reader (Bio-Rad Laboratories, California) (excitation wavelength: 544 nm; emission wavelength: 590 nm). Concentration of rhodamine-labeled LDL in each tissue was calculated using a standard curve and normalized to the weight of the tissue. Equilibrium distribution ratio (K_p value) was measured as the ratio of the concentration of labeled LDL in tissue and in serum ($C_{\text{Tissue}}/C_{\text{Serum}}$ ratio). Graph of K_p versus time was used to observe the slope 6 hours after injection (calculated as $(Y_2 - Y_1)/(X_2 - X_1)$).

Microscopic analysis

Carotid artery, liver, heart and lymph node were cut in $5\mu\text{m}$ thick slices and kept protected from light. Samples were directly mounted and fluorescence was observed under Keyence microscope (BZ-8100, Keyence Corp., Osaka). Immunostaining for ApoB (1:100 dilution, 600-101-111, Rockland Immunochemicals), F4/80 (1:250 dilution, MCA497GA, ABD Serotec) and von Willebrand Factor (1:100 dilution, A0082, DAKO) were done in sections cut within a distance of 5-30 μm from the section where rhodamine-labeled LDL was detected.

RESULTS

We used rhodamine B NHS ester (5-carboxytetraethylrhodamine succinimidyl ester, the structure is shown in Fig. 1A) to label LDL. Rhodamine B NHS ester was constituted by rhodamine B as a main structure and NHS ester which was covalently bound to the amino groups of the protein. Conjugation of Rhodamine B NHS ester with LDL was done at room temperature in sodium bicarbonate buffer. We performed agarose gel electrophoresis to demonstrate that the labeling procedure had not altered lipoprotein integrity (15). Under UV light, labeled LDL clearly appeared (Fig. 1B) suggesting that the fluorescent dye were conjugated. In protein detection staining using Coomassie Brilliant Blue, labeled LDL showed only slightly higher electrophoretic mobility compared to native LDL (Fig. 1C), suggesting that the labeling procedure did not caused any oxidation.

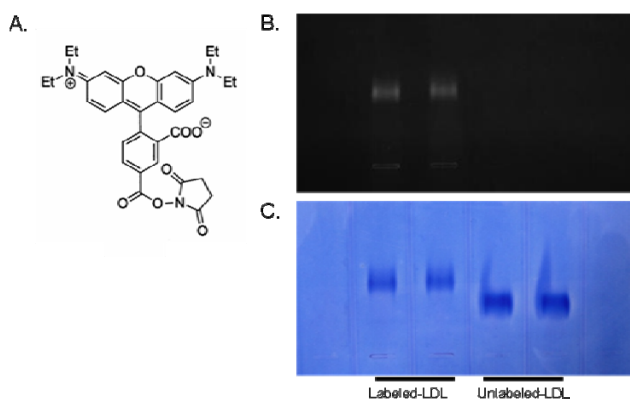


Figure 1.
Rhodamine for the labeling of LDL. (A) The structure of Rhodamine B NHS ester; (B) electrophoresis of unlabeled and labeled-LDL under UV light and (C) after Coomassie Brilliant Blue R-250 staining.

RHODAMINE-LABELED LDL FOR MONITORING LIPOPROTEIN TRAFFIC

Rhodamine-labeled LDL concentration in serum rapidly decreased within two hours after injection. The concentration then slowly decreased from 6 hours to an undetectable level at 50 hours after injection (Fig. 2A). In all tissues, rhodamine-labeled LDL concentration showed a peak at 6 hours, except in adipose tissue where the peak was at 30 minutes (Fig 2A-F). From the $\log[C_{\text{Serum}}]$ versus time graph, we found that the serum level of rhodamine-labeled LDL fell in a monophasic manner with $t_{1/2}$ of 7.69 hours. The evolution of $C_{\text{Tissue}}/C_{\text{Serum}}$ ratio in function of time in each tissue is shown in figure 2G-K. Both in liver and aorta, $C_{\text{Tissue}}/C_{\text{Serum}}$ ratio increased significantly with high slope (0.74 and 0.18 in liver, 0.06 and 0.01 in aorta, at first 2 hours and from 2 until 6 hours after injection, respectively) 6 hours after injection. The increasing of $C_{\text{Tissue}}/C_{\text{Serum}}$ ratio indicated that the LDL was accumulated in tissue. The $C_{\text{Liver}}/C_{\text{Serum}}$ ratio decreased 18 hours after injection, while the $C_{\text{Aorta}}/C_{\text{Serum}}$ ratio still increased. In adipose tissue, kidney and heart, $C_{\text{Tissue}}/C_{\text{Serum}}$ ratio were constant, suggesting that there were a balance between arterial, tissue and venous LDL concentration at each time point. This result also indicated that LDL did not accumulate in adipose tissue, kidney and heart.

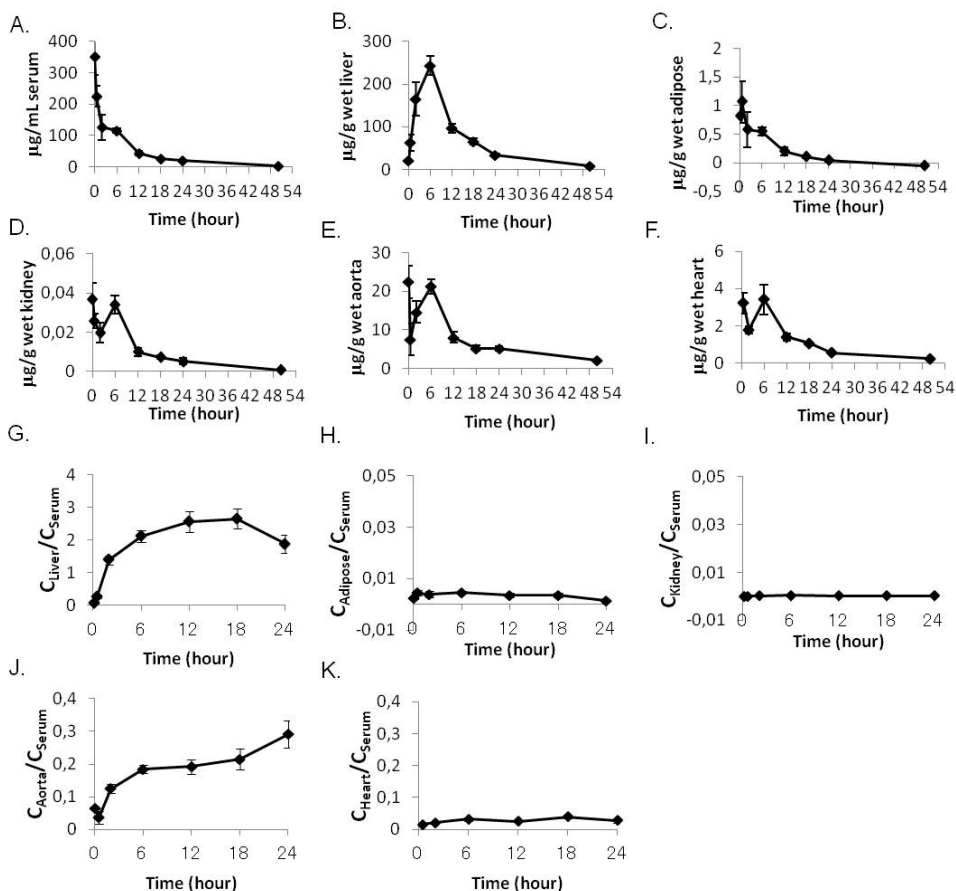


Figure 2. Kinetics of rhodamine-labeled LDL. Rhodamine-labeled LDL concentration in serum (A), liver (B), adipose tissue (C), kidney (D), aorta (E), and heart (F) 1, 30 minutes, 2, 6, 12, 18, 24 and 50 hours after intravenous injection. The ratio of Rhodamine-labeled LDL concentration in tissue and in serum ($C_{\text{Tissue}}/C_{\text{Serum}}$) 1, 30 minutes, 2, 6, 12, 18 and 24 hours after injection in liver (G), adipose tissue (H), kidney (I), aorta (J) and heart (K)

The distribution of rhodamine-labeled LDL in liver, heart and lymph node is shown in figure 3A. Red signal from rhodamine were distributed evenly in all surface of liver from 6 to 18 hours. After 24 hours, the rhodamine signal decreased. In heart, no rhodamine signal was observed at each time point, except inside the vessels (shown at 24 hours). On the other hand, in lymph node, rhodamine-labeled LDL was concentrated in the edge of tissue, which is defined as the superficial cortex. The signal increased from 6 until 18 hours, but it decreased at 24 hours after injection. The binding of rhodamine-LDL in liver was confirmed by the co-localization of rhodamine signal with apoB (Fig. 3B). In liver, rhodamine-LDL was located inside F4/80 positive cells (Fig. 3C), suggesting the uptake of LDL into liver macrophages.

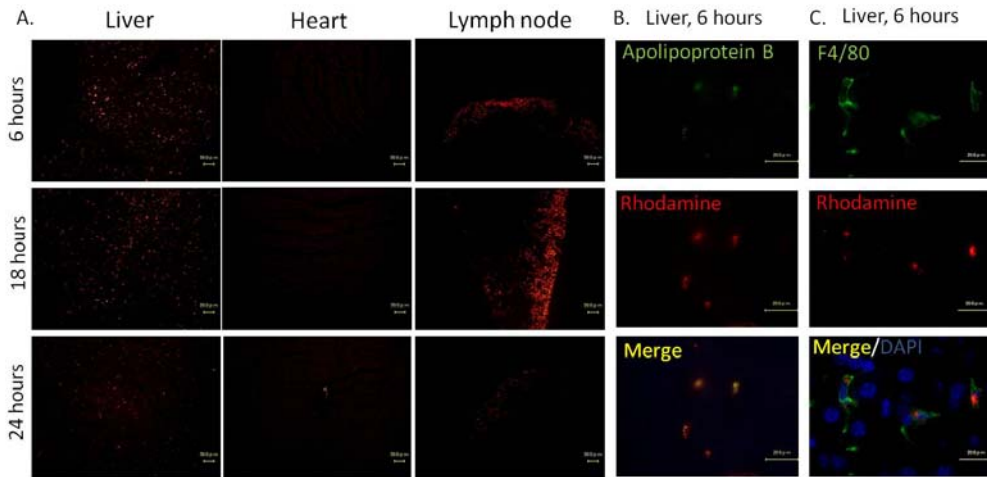


Figure 3. Rhodamine-labeled LDL in liver, heart and lymph node. (A) Distribution of rhodamine-labeled LDL in liver, heart and lymph node 6, 18 and 24 hours after rhodamine-labeled LDL injection. Rhodamine signal co-localized with apolipoprotein B immunofluorescence (B) and inside F4/80 positive cells (C) in liver 6 hours after injection of rhodamine-labeled LDL.

Figure 4A shows the traffic of rhodamine-labeled LDL in ligated carotid artery at 1 minute, 6, 12, 18 and 24 hours after injection. The blue auto-fluorescence was used to identify internal elastic lamina in carotid artery. LDL was visualized in the intimal thickening of the carotid at 6 hours until 18 hours after injection, showed by the red color inside the internal elastic lamina. This result indicated that LDL diffused from lumen through the endothelial cells and was trapped in the intimal thickening at least for 12 hours (from 6 until 18 hours after injection). Twenty four hours after injection, LDL was not observed in the arterial wall anymore. At that time, rhodamine signal was only seen in the lumen of carotid artery. To determine whether the rhodamine signal was located within LDL particles, we determined the location of apoB in carotid artery by immunofluorescence. Figure 4B shows that apoB signals were co-localized with rhodamine indicating that rhodamine B NHS ester was bound with LDL.

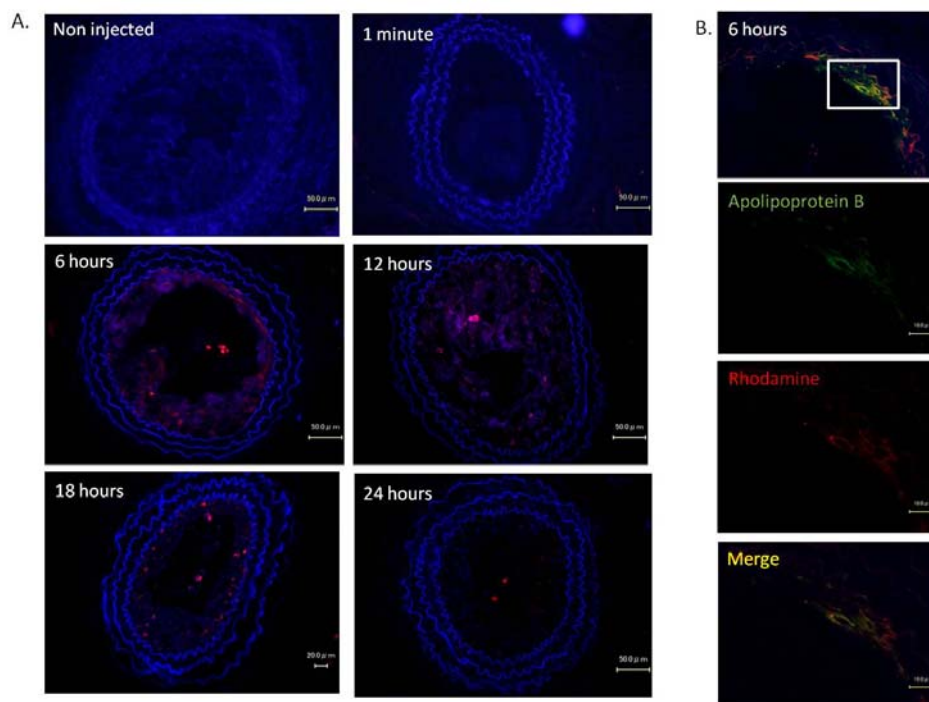


Figure 4. Rhodamine-labeled LDL in carotid artery. (A) Distribution of rhodamine-labeled LDL in carotid ligation of mice 1 minute, 6, 12, 18 and 24 hours after injection. Blue auto-fluorescence was used to identify the structure of carotid artery. (B) Apolipoprotein B immunofluorescence was co-localized with rhodamine signal in carotid artery 6 hours after injection of rhodamine-labeled LDL.

DISCUSSION

This study demonstrated the possibility to use rhodamine-labeled LDL as a tool to observe the retention of lipoproteins in vascular wall intimal thickening in mice. Time course investigation of intravenous bolus of rhodamine-labeled LDL showed the retention of LDL in vascular wall, which corresponded to the initiation of atherosclerosis development.

We first investigated kinetics of rhodamine-labeled LDL in mice. Every drug or solution administered to the body flows in a balance between rate of arterial, tissue and venous concentration. The tissue concentration (C_{Tissue}) increases when the arterial concentration exceeds a rate for which it leaves the venous blood (C_{Serum}) (17). Here we used $C_{\text{Tissue}}/C_{\text{Serum}}$ ratio as an equilibrium distribution ratio, commonly abbreviated as Kp value (17, 18), to observe the relative concentration of rhodamine-labeled LDL in each tissue and each time point.

We confirmed that liver was the main organ to retain rhodamine-labeled LDL, which is consistent with previous reports for LDL kinetics (7, 19-21). The LDL concentration in liver remained high until 18 hours even when the serum concentration decreased, as indicated by the increasing $C_{\text{Liver}}/C_{\text{Serum}}$ ratio. This may indicate that the rhodamine-labeled LDL was transferred actively into the liver through the LDL receptors (19). After 18 hours, the $C_{\text{Liver}}/C_{\text{Serum}}$ ratio decreased, which correlated with the decreasing of red fluorescent signal observed under microscope 24 hours after injection.

Next, we focused on kinetics of rhodamine-labeled LDL in the aorta. Sniderman *et al.* (7) showed that ^{125}I can be detected in aorta only 52 hours after injection. In contrast, we could detect rhodamine-labeled LDL in aorta as early as 30 minutes after administration. The concentration in aorta was at the highest at 6 hours then decreased gradually. However, the ratio of $C_{\text{Aorta}}/C_{\text{Serum}}$ gradually increased, even after 18 hours. The transfer of LDL into the aorta occurs independently of LDL receptors (22), and the relationship between serum LDL concentration and influx of LDL into the aorta is linear (23). The increasing of the slope in the ratio of $C_{\text{Aorta}}/C_{\text{Serum}}$ strongly indicated that the rhodamine-labeled LDL was actively trapped in the aorta. Taken together, those kinetics both in the liver and in the aorta indicated that the rhodamine-labeled LDL exhibited a similar behavior as the native LDL, and that it was a sensitive tool to observe the distribution in details in the aorta.

The carotid artery is prone to atherosclerosis because of the high shear stress due to the disturbance of blood flow near the carotid bifurcation. Complete ligation near the bifurcation induces rapid proliferation of smooth muscle cells, leading to extensive neointima formation with preserved endothelial cell layer (24). In the present study, neointima formation was used to mimic the early human atherosclerosis, which is usually called DIT. Because most laboratory animals do not develop distinct DIT like humans do, we induced the proliferation of smooth muscle cells by performing carotid ligation. An alternative procedure consists in mechanically inducing endothelial denudation by passing a flexible wire through the carotid artery (25). However, using this method, the denudation of endothelial cells increases the uptake and the removal of LDL in the arterial wall (8, 26). It seems that the diffusion of lipoproteins through the arterial wall in the mechanically induced endothelial cells denudation model does not mimic the human DIT. Therefore, we performed carotid ligation to achieve DIT without denudation of endothelial cells. We confirmed that the endothelial cell layer was preserved in the ligated carotid artery (Fig. 5).

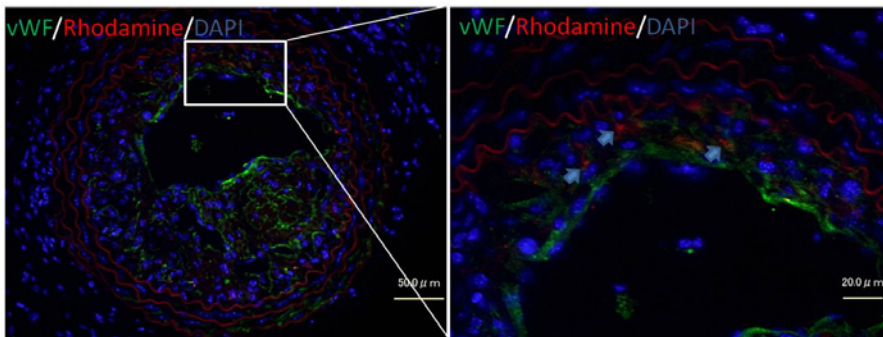


Figure 5. Intact endothelial cells showed by the expression of von Willebrand Factor in the lumen side of intimal thickening. Rhodamine-labeled LDL (showed by arrows) appeared as the red color inside the intimal thickening.

Labeled LDL was visualized in intimal thickening of carotid artery from 6 hours until 18 hours after injection inside the internal elastic lamina (Fig. 4A). This observation indicates that labeled LDL was specifically trapped in DIT and that the amount of trapped labeled LDL was sufficient to be seen by a microscopy analysis. Retention of LDL in arterial wall is promoted by the elongation of CS chains in proteoglycan (5). The modification of CS chains length could therefore be indirectly observed by using injection of labeled LDL.

RHODAMINE-LABELED LDL FOR MONITORING LIPOPROTEIN TRAFFIC

Retention of lipoprotein in arterial wall is not only due to the high concentration of serum LDL, but also to the reduction of lipoprotein egress (1, 27). The efflux route of LDL is the endothelial cells, through which they reach back the lumen (28). In this study, reduction of lipoprotein in arterial wall began 24 hours after injection of rhodamine-labeled LDL. The decreasing of labeled LDL can be explained by the egress of lipoprotein, meaning that LDL was leaving the arterial wall to the lumen.

Taken together, injection of rhodamine-labeled LDL would be a useful method to analyze the trapping of LDL in the arterial wall. Based on the "response-to-retention" hypothesis, this method may be applied in investigating the mechanisms of the early phase of atherosclerosis in mice which underwent carotid ligation. Moreover, given that trapping of LDL is promoted by the elongation of CS chains in the arterial wall, this procedure may be an indirect tool to assess the size of CS chains. Finally, injection of rhodamine-labeled LDL may become a breakthrough method to identify whether the arterial wall is prone to atherosclerosis.

ACKNOWLEDGEMENT

We thank Dr. Kumiko Ueda for her helpful discussion on the kinetics study of labeled LDL.

REFERENCES

1. **Williams, K.J., Tabas, I.** 1995. The Response-to-Retention Hypothesis of Early Atherogenesis. *Arterioscler Thromb Vasc Biol* **15**:551-561
2. **Dadlani, H., Ballinger, M.L., Osman, N., Getachew, R., Little, P.J.** 2008. Smad and p38 MAP Kinase-mediated Signaling of Proteoglycan Synthesis in Vascular Smooth Muscle. *J Biol Chem* **283**:7844-7852
3. **Getachew, R., Ballinger, M.L., Burch, M.L., Reid, J.J., Khachigian, L.M., Wight, T.N., Little, P.J., Osman, N.** 2010. PDGF β -Receptor Kinase Activity and ERK1/2 Mediate Glycosaminoglycan Elongation on Biglycan and Increases Binding to LDL. *Endocrinology* **151**:4356-4367
4. **Chang, M.Y., Potter-Perigo, S., Tsoi, C., Chait, A., Wight, T.N.** 2000. Oxidized low density lipoproteins regulate synthesis of monkey aortic smooth muscle cell proteoglycans that have enhanced native low density lipoprotein binding properties. *J Biol Chem* **275**:4766-4773
5. **Little, P.J., Ballinger, M.L., Burch, M.L., Osman, N.** 2008. Biosynthesis of natural and hyperelongated chondroitin sulfate glycosaminoglycans: new insights into an elusive process. *Open Biochem J* **2**:135-142
6. **Anggraeni, V.Y., Emoto, N., Yagi, K., Mayasari, D.S., Nakayama, K., Izumikawa, T., Kitagawa, H., Hirata, K-i.** 2011. Correlation of C4ST-1 and ChGn-2 expression with chondroitin sulfate chain elongation in atherosclerosis. *Biochem Biophys Res Commun* **406**:36-41
7. **Sniderman, A.D., Carew, T.E., Steinberg, D.** 1975. Turnover and tissue distribution of 125-I-labeled low density lipoprotein in swine and dogs. *J Lipid Res* **16**:293-299
8. **Preobrazhensky, S.N., Dolgov, V.V., Flegel, H.G., Repin, V.S., Smirnov, V.N.** 1983. [125I]LDL uptake in rabbit arteries perfused in situ effect of HDL on intact and de-endothelialized vessels. *Atherosclerosis* **48**:147-155
9. **Davis, W., Haugland, R.** 1995. Coupling of Monoclonal Antibodies with Fluorophores. In: *Monoclonal Antibody Protocols*: Humana Press; 205-221

10. **Boyarskiy, V.P., Belov, V.N., Medda, R., Hein, B., Bossi, M., Hell, S.W.** 2008. Photostable, Amino Reactive and Water-Soluble Fluorescent Labels Based on Sulfonated Rhodamine with a Rigidized Xanthene Fragment. *Chemistry –Eur J* **14**:1784-1792
11. **Koide, Y., Urano, Y., Kenmoku, S., Kojima, H., Nagano, T.** 2007. Design and Synthesis of Fluorescent Probes for Selective Detection of Highly Reactive Oxygen Species in Mitochondria of Living Cells. *J Am Chem Soc* **129**:10324-10325
12. **Gordiyenko, N., Campos, M., Lee, J.W., Fariss, R.N., Sztein, J., Rodriguez, I.R.** 2004. RPE Cells Internalize Low-Density Lipoprotein (LDL) and Oxidized LDL (oxLDL) in Large Quantities In Vitro and In Vivo. *Invest Ophthalmol Vis Sci* **45**:2822-2829
13. **Hummel, S., Lynn, E.G., Osanger, A., Hirayama, S., Nimpf, J., Schneider, W.J.** 2003. Molecular characterization of the first avian LDL receptor. *J Lipid Res* **44**:1633-1642
14. **Cano, M., Fijalkowski, N., Kondo, N., Dike, S., Handa, J.** 2011. Advanced Glycation Endproduct Changes to Bruch's Membrane Promotes Lipoprotein Retention by Lipoprotein Lipase. *Am J Pathol* **179**:850-859
15. **Hofer, G., Steyrer, E., Kostner, G.M., Hermetter, A.** 1997. LDL-mediated interaction of Lp[a] with HepG2 cells: a novel fluorescence microscopy approach. *J Lipid Res* **38**:2411-2421
16. **Hermanson, G.T.** 2008. *Bioconjugate Techniques*. second ed. Boston: Elsevier Inc.
17. **Rowland, M., Tozer, T.N.** 1995. *Clinical Pharmacokinetics: Concepts and Applications*. third ed: Williams & Wilkins
18. **Björkman, S.** 2005. A Comment on the Application of Drug Tissue-Plasma Partition Coefficients K_p in Eliminating Organs to Calculation of Volume of Distribution at Steady State. *Journal of Pharmacokinetics and Pharmacodynamics* **32**:655-658
19. **Kamps, J.A., Kruijt, J.K., Kuiper, J., Van Berkel, T.J.** 1991. Uptake and degradation of human low-density lipoprotein by human liver parenchymal and Kupffer cells in culture. *Biochem J* **276**:135-140
20. **Rudling, M.J., Reihner, E., Einarsson, K., Ewerth, S., Angelin, B.** 1990. Low density lipoprotein receptor-binding activity in human tissues: quantitative importance of hepatic receptors and evidence for regulation of their expression in vivo. *Proc Natl Aca Sci USA* **87**:3469-3473
21. **Nenseter, M.S., Gudmundsen, O., Roos, N., Maelandsmo, G., Drevon, C.A., Berg, T.** 1992. Role of liver endothelial and Kupffer cells in clearing low density lipoprotein from blood in hypercholesterolemic rabbits. *J Lipid Res* **33**:867-877
22. **Wiklund, O., Carew, T.E., Steinberg, D.** 1985. Role of the low density lipoprotein receptor in penetration of low density lipoprotein into rabbit aortic wall. *Arterioscler Thromb Vasc Biol* **5**:135-141
23. **Nordestgaard, B.G., Tybjaerg-Hansen, A., Lewis, B.** 1992. Influx in vivo of low density, intermediate density, and very low density lipoproteins into aortic intimas of genetically hyperlipidemic rabbits. Roles of plasma concentrations, extent of aortic lesion, and lipoprotein particle size as determinants. *Arterioscler Thromb Vasc Biol* **12**:6-18
24. **Kumar, A., Lindner, V.** 1997. Remodeling With Neointima Formation in the Mouse Carotid Artery After Cessation of Blood Flow. *Arterioscler Thromb Vasc Biol* **17**:2238-2244
25. **Lindner, V., Fingerle, J., Reidy, M.A.** 1993. Mouse model of arterial injury. *Circ Res*

RHODAMINE-LABELED LDL FOR MONITORING LIPOPROTEIN TRAFFIC

73:792-796

26. **Alavi, M., Moore, S.** 1984. Kinetics of low density lipoprotein interactions with rabbit aortic wall following balloon catheter deendothelialization. *Arterioscler Thromb Vasc Biol* **4**:395-402
27. **Tabas, I., Williams, K.J., Borén, J.** 2007. Subendothelial Lipoprotein Retention as the Initiating Process in Atherosclerosis: Update and Therapeutic Implications. *Circulation* **116**:1832-1844
28. **Nordestgaard, B.G., Hjelms, E., Stender, S., Kjeldsen, K.** 1990. Different efflux pathways for high and low density lipoproteins from porcine aortic intima. *Arterioscler Thromb Vasc Biol* **10**:477-485